Available online at www.sciencedirect.com
SCIENCE DIRECT
Journal of Molecular Structure 742 (2005) 43–48
Journal of MOLECULAR STRUCTURE
www.elsevier.com/locate/molstruc

Coulomb explosion imaging: the CH_3^+ and H_3O^+ molecules

S.N. Yurchenko[a,1], P.R. Bunker[a], Per Jensen[b,*]

[a]*Steacie Institute for Molecular Sciences, National Research Council of Canada, Ottawa, Ont., Canada K1A 0R6*
[b]*Theoretische Chemie, Bergische Universität, D-42097 Wuppertal, Germany*

Received 24 September 2004; revised 20 November 2004; accepted 22 November 2004
Available online 17 February 2005

In honor of Dr Walter Lafferty for his many contributions to science

Abstract

We calculate the thermally averaged probability distribution for the out-of-plane inversion motion of the CH_3^+ and H_3O^+ molecules. Such distributions can be obtained experimentally by using Coulomb explosion imaging (CEI) techniques, and our results will be useful in the interpretation of such images. We calculate these probability distributions from the molecular wavefunctions that we obtain by solving variationally the nine-dimensional rotation–vibration Schrödinger equation using the recently developed 'XY_3' Hamiltonian and computer program.

Keywords: Coulomb explosion imaging; Large amplitude vibration; Inversion; Molecular ions; Spectroscopy; CH_3^+; H_3O^+; Carbo-ions

1. Introduction

Previous Coulomb explosion imaging (CEI) work that we have been involved with is concerned with triatomic molecules such as CH_2^+ [1–3] and D_2O [4]. Experimentally, there are two different CEI techniques: either one accelerates a molecule (usually a molecular ion) through a thin foil (see, for example, Ref. [5]), or one subjects the molecule (usually a neutral molecule) to an intense few-cycle laser pulse (see, for example, Ref. [4]). In either case, several electrons are stripped off the target molecule in a very short time interval, and the resultant highly electron-deficient system 'Coulomb-explodes'; the fragments are imaged, and the structure of the molecule at the instant of the 'explosion' is inferred.

Our RENNER computer program [6] was used, with accurate analytic three-dimensional potential energy surfaces for the $\tilde{X}$ and $\tilde{A}$ states of the CH_2^+ ion, to determine molecular rovibronic wavefunctions. In Ref. [1], these rovibronic wavefunctions were used to determine the thermally averaged bending probability distribution at room temperature. This distribution was calculated for use in simulating the result of CEI experiments on CH_2^+, in particular the thin-foil CEI experiment reported in Ref. [7]. The bending probability curve calculated theoretically for CH_2^+ in Ref. [1] deviated considerably from the experimental curve determined in Ref. [7]. We investigated in Ref. [1] possible reasons for the lack of agreement, considering both a theoretical error in the calculation of the shape of the ground state potential energy surface, or in the neglect of all electronic states other than $\tilde{X}^2A$ and $\tilde{A}^2B$, and an experimental error in determining the temperature of the ions. The effect of temperature, and of excited electronic states, were shown to be negligible in Ref. [1], and it was also shown that the change in the shape of the ground state potential energy surface that was required in order to explain the discrepancy was improbably large in view of the level of the ab initio calculation used to obtain it.

Because of the discrepancy new thin-foil CEI experiments on CH_2^+ were carried out at the Test Storage Ring Facility (TSR) at the Max Planck Institute of Nuclear Physics in Heidelberg; the results are now published [5,8].

* Corresponding author. Tel.: +49 202 439 2468; fax: +49 202 439 2509.
E-mail address: jensen@uni-wuppertal.de (P. Jensen).
[1] Present address: Max-Planck-Institut für Kohlenforschung, D-45470 Mülheim an der Ruhr, Germany.

0022-2860/$ - see front matter © 2005 Elsevier B.V. All rights reserved.
doi:10.1016/j.molstruc.2004.11.092

To assist with the interpretation of these new CEI experiments, the authors of Ref. [1] provided the authors of Ref. [5] with a theoretical prediction of the thermally averaged probability distribution for the bending angle. The data were transferred in the form of a computer file giving the values of the probability density function at a grid of equidistantly spaced bond angle values. This bending probability distribution was used as the starting point for simulating the results of the new CEI experiments. In the simulation it was necessary to use Monte Carlo methods to describe the interaction between the fragments of the exploding molecule and the particles of the thin foil; this makes the result of the CEI experiment differ in a systematic way from the bending probability distribution obtained directly from the molecular wavefunctions as described in Ref. [1]. Preliminary results of the simulations, and the experimental CEI data, were kindly made available by Lammich and co-workers [5,8], so that it could be published in Fig. 2 of Ref. [3]. Very recently, the final results of the simulations have been compared to the experimental data in Fig. 7 of Ref. [5]. Unfortunately, it is not clearly stated in Ref. [5] that the simulations in Fig. 7 of Ref. [5] are based on the room-temperature bending probability distribution for CH_2^+ calculated theoretically in Ref. [1].

As shown by Fig. 7 of Ref. [5], the experimental CEI result for CH_2^+ is in agreement with the theoretical prediction from Ref. [1], to within the uncertainties inherent in the CEI method. This shows that all significant systematic errors in the beam-foil CEI experiment for CH_2^+ can be accounted for.

The result obtained in Ref. [5] gives encouragement for the credibility of future CEI results, and shows how useful a theoretical simulation of a geometric probability distribution can be. In the present work we extend the calculations to four-atomic XY_3 molecules. We simulate the thermally averaged out-of-plane inversion probability distribution of the (planar) CH_3^+ and (inverting) H_3O^+ molecular ions. The aim of this work is to challenge further the precision of the CEI technique for molecules larger than triatomic, with the ultimate goal of helping in the production of accurately interpreted CEI results for larger molecules such as CH_5^+.

2. Inversion angle probability distributions

Coordinate probability distributions are calculated using molecular wavefunctions. For an XY_3 molecule, within the Born–Oppenheimer approximation, the required wavefunctions are obtained by diagonalizing the nine-dimensional rotation–vibration Hamiltonian. To do this for the H_3O^+ and CH_3^+ molecules we use the 'XY_3' Hamiltonian and computer program that is developed and described in Refs. [9,10]; the way the XY_3 Hamiltonian is set up, and the procedure used to diagonalize it, is an extension of the MORBID treatment used for triatomic molecules [11]. The XY_3 Hamiltonian is set up and diagonalized in a basis set; each basis set function is the product of a symmetric top rotational function $|J, k, m\rangle$, three local-mode Morse oscillator stretching functions $|v_1\rangle|v_2\rangle|v_3\rangle$, a numerical inversion function $|v_{\rm inv}\rangle$ obtained in a preliminary Numerov–Cooley integration of the inversion Schrödinger equation, and a two-dimensional isotropic harmonic oscillator bending function $|v_4, l_4\rangle$. The rotation–vibration wavefunctions $\Phi_{\rm rv}$ are thus obtained as linear combinations of these product basis functions. The potential energy function is expanded as in Ref. [9]:

$$V(\xi_1,\xi_2,\xi_3,\xi_{4a},\xi_{4b};\sin\bar{\rho}) = V_{\rm e} + V_0(\sin\bar{\rho}) + \sum_j F_j(\sin\bar{\rho})\xi_j + \sum_{j\le k} F_{jk}(\sin\bar{\rho})\xi_j\xi_k + \sum_{j\le k\le l} F_{jkl}(\sin\bar{\rho})\xi_j\xi_k\xi_l + \sum_{j\le k\le l\le m} F_{jklm}(\sin\bar{\rho})\xi_j\xi_k\xi_l\xi_m\ldots \quad (1)$$

This analytical function is expressed in terms of the variables

$$\xi_k = 1 - \exp(-a(r_k - r_{\rm e})), \quad k = 1,2,3, \quad (2)$$

$$\xi_{4a} = \frac{1}{\sqrt{6}}(2\alpha_{23} - \alpha_{13} - \alpha_{12}), \quad (3)$$

$$\xi_{4b} = \frac{1}{\sqrt{2}}(\alpha_{13} - \alpha_{12}), \quad (4)$$

where r_k, $k=1$, 2, 3, is the instantaneous value of the distance between the 'central' nucleus (C for CH_3^+ and O for H_3O^+) and the proton labeled k, and the bond angle $\alpha_{kl} = \angle(H_kXH_l)$, k, $l=1$, 2, 3, where X is the central nucleus. Further,

$$\sin\bar{\rho} = \frac{2}{\sqrt{3}}\sin(\bar{\alpha}/2), \quad (5)$$

where $\bar{\alpha} = (\alpha_{12} + \alpha_{23} + \alpha_{13})/3$ is the average of the bond angles. The pure inversion potential energy function in Eq. (1) is

$$V_0(\sin\bar{\rho}) = \sum_s f_0^{(s)}(\sin\rho_{\rm e} - \sin\bar{\rho})^s, \quad (6)$$

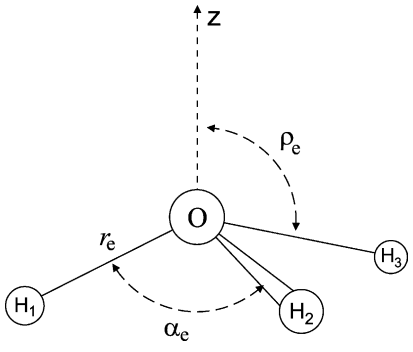

Fig. 1. The definition of the equilibrium parameters ρ_e, α_e, and r_e.

Table 1
The potential energy function parameters[a] for CH_3^+

Parameter	Value
ρ_e (deg)	90.0
r_{14}^e (Å)	1.08839
a (Å^{-1})	1.86
V_e	0.0
f_0^1	165,271.4 (51)[b]
f_0^2	41,974 (209)
f_0^3	72,227 (2862)
f_0^4	−439,795 (12,858)
f_1^1	−22,698.3 (89)
f_1^2	3987 (232)
f_1^3	43,498 (1494)
f_{11}^0	39,631.2 (11)
f_{11}^1	−19,551 (52)
f_{11}^2	−21,304 (1214)
f_{11}^3	47,339 (7795)
f_{13}^0	−306.2 (11)
f_{13}^1	7001 (36)
f_{13}^2	−12,775 (348)
f_{4a4a}^0	10,045.75 (74)
f_{4a4a}^1	20,857 (43)
f_{4a4a}^2	−62,333 (820)
$f_{14a}^0\sqrt{3/2}$	−1938.9 (21)
$f_{14a}^1\sqrt{3/2}$	−6799 (85)
$f_{14a}^2\sqrt{3/2}$	18,364 (1157)
f_{111}^0	−391 (57)
f_{111}^1	−4368 (111)
f_{113}^0	−38.8 (33)
f_{113}^1	4174 (112)
f_{113}^2	−10,031 (1062)
f_{123}^0	−215 (87)
f_{123}^1	−29,405 (369)
f_{123}^2	32,670 (3484)
f_{4a4a4a}^0	−1561 (13)
f_{4a4a4a}^1	−10,186 (124)
f_{4a4a4a}^2	12,882 (2422)
$f_{114a}^0\sqrt{3/2}$	−1222.4 (82)
$f_{114a}^1\sqrt{3/2}$	1361 (197)
$f_{134b}^0\sqrt{2}$	−2572.4 (65)
$f_{134b}^1\sqrt{2}$	3166 (174)
$f_{14a4a}^0+f_{24a4b}^0/\sqrt{3}$	−2292.3 (94)
$f_{14a4a}^1+f_{24a4b}^1/\sqrt{3}$	3276 (28)
$-f_{24a4b}^0/\sqrt{2}$	1356.8 (27)
$-f_{24a4b}^1/\sqrt{2}$	−1605 (101)
f_{1111}^0	5812 (23)
f_{1111}^1	−6452 (379)
f_{1113}^0	206 (10)
f_{1133}^0	−837 (14)
f_{1123}^0	−1110 (13)
$f_{114a4a}^0+f_{224a4b}^0/\sqrt{3}$	7705.6 (44)
$-f_{224a4b}^0/\sqrt{2}$	−6866 (12)
$f_{134a4a}^0-f_{134a4b}^0/\sqrt{12}$	1395.5 (39)
$-f_{134a4b}^0/\sqrt{2}$	12,602.5 (85)
$f_{1114a}^0\sqrt{3/2}$	−519 (29)
$f_{4a4a4a4a}^0$	571.8 (33)
$-f_{1334b}^0\sqrt{2}$	1141 (17)
$f_{1124b}^0\sqrt{2}$	1278 (16)
$f_{14a4a4a}^0-2f_{24a4a4b}^0/\sqrt{3}$	213.4 (14)
$f_{24a4a4b}^0\sqrt{2}$	−476.1 (91)

[a] In cm^{-1} unless otherwise stated.
[b] The number in parentheses is one standard error in units of the last digit quoted; parameters without a standard error were held fixed.

and the functions $F_{jk\ldots}(\sin\bar{\rho})$ are defined as

$$F_{jk\ldots}(\sin\bar{\rho}) = \sum_s f_{jk\ldots}^{(s)}(\sin\rho_e - \sin\bar{\rho})^s \quad (7)$$

where $\sin\rho_e$ is the equilibrium value of $\sin\bar{\rho}$ (see Fig. 1), a is the Morse oscillator exponent parameter, and the quantities $f_0^{(s)}$ and $f_{jk\ldots}^{(s)}$ in Eqs. (6) and (7) are expansion coefficients. The (very small) difference between the instantaneous inversion coordinate $\bar{\rho}$ and the angle ρ that occurs in the Hamiltonian is explained in Ref. [9]. To carry out the calculation of the wavefunctions for the H_3O^+ and CH_3^+ molecules we need potential energy surfaces.

For the CH_3^+ molecule we use the ab initio potential V of Yu and Sears [12]; this potential gives a planar D_{3h} equilibrium structure with $R(CH) = 1.088$ Å. The analytical function for V in Ref. [12] is different from that required in the XY_3 computer program. This made it necessary for us first to use the results of Ref. [12] to calculate V at an even grid of 2610 values (with energies up to about 2.2 eV above equilibrium). We then obtained the values of the parameters in our analytical function by making a least squares fitting of the function to the values of V at these grid points. The root-mean-square (rms) deviation of the fitting was 0.6 cm^{-1}. The optimum values of the parameters are given in Table 1. Using this potential in the XY_3 program to calculate vibrational ($J=0$) energies, we obtain energies that have an rms deviation of 3.1 cm^{-1} when compared to the 65 calculated vibrational energies given in Table 2 of Ref. [12] for the CH_3^+ isotopomer. In this variational calculation the expansions of the kinetic energy factors $G_{\alpha\beta}$ and the pseudo-potential U were taken to 4th order, and the potential energy V to 6th order; the basis set was truncated so that

$$P = 2(v_1 + v_2 + v_3) + v_{inv} + v_4 \leq 14, \quad (8)$$

where v_1, v_2 and v_3 are the local mode Morse oscillator stretching quantum numbers, v_{inv} is the inversion quantum number, and v_4 is the bending quantum number. The limit $P \leq 14$ means that the sizes of the symmetrized basis sets were $N(A_1) = 1455$, $N(A_2) = 1125$ and $N(E) = 2571$. In the numerical integration of the inversion Schrödinger equation a grid of 1000 points was used.

In order to make calculations that include rotation we have to reduce the size of the vibrational basis set given in Eq. (8) to keep the calculation tractable. After some trials we found it satisfactory to use $P \leq 6$, and to limit the expansions of the $G_{\alpha\beta}$ and U to 2nd order, and of V to 4th order. Comparing the $J=0$ energies obtained in this

Table 2
The potential energy function parameters[a] for H_3O^+

Parameter	Value
ρ_e (deg)	107.105 (52)[b]
r_e (Å)	0.978039 (96)
a (Å^{-1})	2.5
V_e	−16,798,969.0 (41)
f_0^2	351,437 (2113)
f_0^3	−521,237 (67,093)
f_0^4	1,056,173 (404,737)
f_1^1	−23,499 (337)
f_{11}^0	31,063 (121)
f_{11}^1	−13,555 (3751)
f_{4a4a}^0	14,916 (48)
f_{4a4a}^1	69,617 (4076)
f_{4a4a4a}^0	−1709 (234)
$f_{114a}^0\sqrt{3/2}$	37,401 (12,451)
f_{14a4a}^0	−3461 (443)

[a] In cm^{-1} unless otherwise stated.
[b] The number in parentheses is one standard error in units of the last digit quoted; parameters without a standard error were held fixed.

calculation with those obtained in the larger calculation reported above, we found that for the eight vibrational levels below 4000 cm^{-1} the rms deviation was only 2 cm^{-1}. Vibrational levels above 4000 cm^{-1} contribute insignificantly to the room temperature inversion probability distribution. In the calculation the maximum J value used was $J=10$. In tests it was found that the rms difference between the distributions calculated using maximum J values of 9 and 10 was only 5×10^{-5} for CH_3^+, and so we did not include states with $J>10$.

For the H_3O^+ molecule we determined the parameters in V by making a least squares fitting to the 61 ab initio energies in Ref. [13]. The optimum values of the parameters are given in Table 2. The equilibrium geometry and inversion barrier height [R(OH) = 0.978 Å, α(HOH) = 111.6° and H = 712 cm^{-1}] are negligibly different from those obtained in a more recent CCSD(T) aug-cc-pVQZ ab initio calculation [14] [0.977 Å, 111.7° and 706 cm^{-1}]. The variational calculation of the vibrational energies yielded the results given in Table 3, and we see that they are similar to those obtained in Ref. [14] (see the results under the headings HCB-2 and HCB-3 for H_3O^+ in Table 3 of Ref. [14]). In our variational calculation we used $P\leq10$, and limited the expansions of the $G_{\alpha\beta}$ and U to 4th order, and of V to 6th order. For the calculation including rotation it was satisfactory to use $P\leq6$, and to limit the expansions of the $G_{\alpha\beta}$ and U to 2nd order, and of V to 4th order. It was necessary to make calculations up to $J=15$ to obtain a converged inversion probability distribution; the rms difference between the distributions calculated using maximum J values of 14 and 15 was only 3×10^{-5}, and so we did not include states with $J>15$. The vibrational energies reported in Table 3 of Ref. [13] are not in very close agreement with the results obtained here despite the fact that both calculations are based on the same set of ab initio potential energy points. This is due to inadequacies in the nonrigid invertor Hamiltonian used in Ref. [13], which is based on the use of Van Vleck perturbation theory for all vibrational modes except the inversion.

Table 3
Calculated vibrational wavenumbers in cm^{-1} for H_3O^+

State	ν
ZPE	7498
0(−)	41
ν_2(+)	599
ν_2(−)	937
$2\nu_2$(+)	1450
$2\nu_2$(−)	2004
ν_4(+)	1607
ν_4(−)	1654
ν_1(+)	3330
ν_1(−)	3363
ν_3(+)	3479
ν_3(−)	3509

3. Results

We calculate the thermally averaged out-of-plane inversion angle distributions for the H_3O^+ and CH_3^+ molecules as a function of temperature. These can be used to simulate the results of CEI experiments as done for CH_2^+ in Fig. 2 of Ref. [3] and in Fig. 7 of Ref. [5]. To make the calculation we follow the procedure discussed in Section 2 of Ref. [1] which explains how the thermally averaged bending angle distribution for the CH_2^+ molecule is obtained. The reader is referred to Ref. [1] for more details since we only discuss here the parts of that calculation that are changed for these two XY_3 molecules. For CH_2^+ it is necessary to use rovibronic wavefunctions that incorporate the breakdown of the Born–Oppenheimer approximation caused by the Renner–Teller interaction, and also to include the effect of spin–orbit coupling. For H_3O^+ and CH_3^+ we can safely work within the Born–Oppenheimer approximation and neglect spin–orbit coupling since there are no low lying excited electronic states. As a result we do not

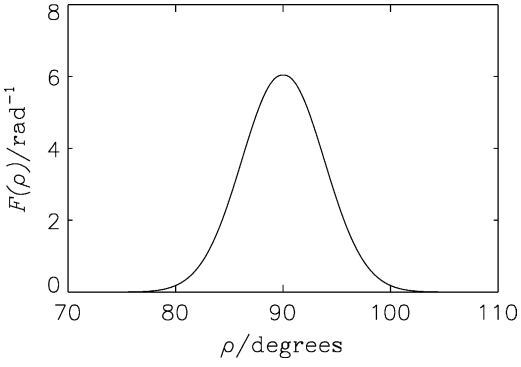

Fig. 2. The thermally averaged out-of-plane bending probability distribution $F(\rho)$ for CH_3^+ at 300 K.

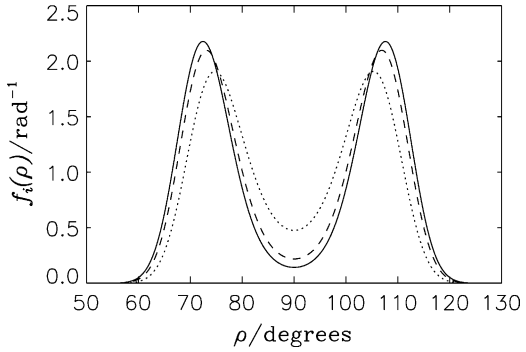

Fig. 3. The single state inversion probability distribution functions $f_i(\rho)$ for the 0^+ ground vibrational state levels of H_3O^+ with $J=15$ and $K=3$ (solid line), $K=9$ (dashed line) and $K=15$ (dotted line).

need to consider the electronic wavefunction and can simply use the rotation–vibration wavefunctions $\Phi_{\rm rv}$ obtained by diagonalizing the XY_3 Hamiltonian.

The normalized inversion coordinate probability density function $f(\rho)$ for a given state is obtained by integrating the square of $\Psi_{\rm rv}$ over all coordinates except the out-of-plane inversion coordinate ρ (i.e. over the rotation, stretching, and bending coordinates). Thus,

$$f(\rho) = \int {\rm d}V |\Psi_{\rm rv}|^2, \tag{9}$$

where dV is the volume element for the rotation, stretching, and bending coordinates. To evaluate this integral for each state we use the eigenvector coefficients obtained from the XY_3 Hamiltonian diagonalization procedure, and make use of the fact that the rotation, stretching and bending functions in the basis each form orthonormal sets.

An arbitrary energy level E_i will have a total degeneracy of g_i. This degeneracy is the product of the $(2J+1)$ m-degeneracy and the nuclear spin degeneracy $g_{\rm ns}$. For the $^{12}CH_3^+$ or $H_3^{16}O^+$ isotopomers that we consider here $g_{\rm ns}=0$ for levels having symmetry A_1' or A_1'' ('missing' levels), $g_{\rm ns}=2$ for *para* levels having symmetry E' or E'', and $g_{\rm ns}=4$ for *ortho* levels having symmetry A_2' or A_2''. The g_i rovibrational nuclear-spin wavefunctions belonging to the particular level E_i will all have the same inversion

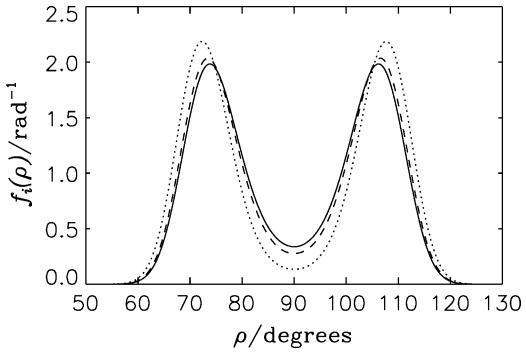

Fig. 4. The single state inversion probability distribution functions $f_i(\rho)$ for the 0^+ ground vibrational state levels of H_3O^+ with $K=0$ and $J=1$ (solid line), $J=7$ (dashed line) and $J=15$ (dotted line).

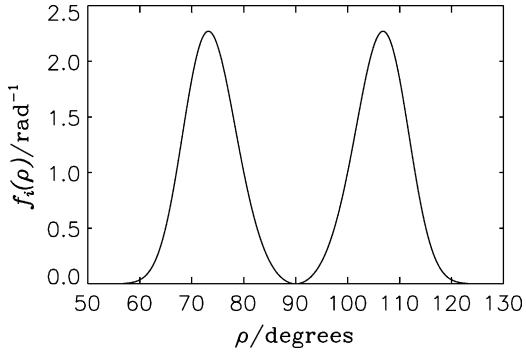

Fig. 5. The single state inversion probability distribution function $f_i(\rho)$ for the 0^- vibrational state levels of H_3O^+ with $J=0$.

probability density function $f_i(\rho)$. As a result, for an ensemble of CH_3^+ or H_3O^+ molecules in thermal equilibrium at absolute temperature T, the thermally averaged inversion probability density function $F(\rho)$ is proportional to the Boltzmann-factor-weighted sum of the $f_i(\rho)$, i.e.

$$F(\rho) \propto \sum_i g_i \exp\left(-\frac{E_i}{kT}\right) f_i(\rho), \tag{10}$$

where k is the Boltzmann constant. Since the total probability over all ρ values is unity, $F(\rho)$ must be such that its integral over ρ is unity. Thus the normalized expression for the distribution function $F(\rho)$ is

$$F(\rho) = \sum_i g_i \exp\left(-\frac{E_i}{kT}\right) f_i(\rho) \Big/ \int \sum_i g_i \exp\left(-\frac{E_i}{kT}\right) f_i(\rho) {\rm d}\rho, \tag{11}$$

which is equivalent to dividing by the partition function; in the summation we choose the highest E_i so that there is satisfactory convergence.

In Fig. 2 we show the thermally averaged out-of-plane inversion probability distribution $F(\rho)$ for the planar CH_3^+ molecular ion at 300 K that we obtain by using Eq. (11). The result for $T=30$ K is not noticeably different on the scale of Fig. 2. For the inverting H_3O^+ molecular ion we show in Figs. 3–5 some single state inversion probability functions $f_i(\rho)$ calculated using Eq. (9), and in Fig. 6 we show the

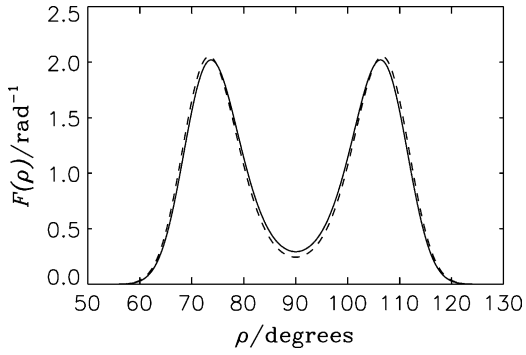

Fig. 6. The thermally averaged out-of-plane inversion probability distribution $F(\rho)$ for H_3O^+ at 30 (solid line) and 300 K (dashed line).

thermally averaged distribution $F(\rho)$ for H_3O^+ at 30 and 300 K. Experimental CEI simulations for CH_3^+ and H_3O^+ can be obtained using these $F(\rho)$ functions.

Acknowledgements

The work of P.J. is supported in part by the Deutsche Forschungsgemeinschaft and the Fonds der Chemischen Industrie.

References

[1] G. Osmann, P.R. Bunker, W.P. Kraemer, P. Jensen, Chem. Phys. Lett. 309 (1999) 299.
[2] G. Osmann, P.R. Bunker, W.P. Kraemer, P. Jensen, Chem. Phys. Lett. 318 (2000) 597.
[3] P. Jensen, T.E. Odaka, W.P. Kraemer, T. Hirano, P.R. Bunker, Spectrochim. Acta A 58 (2002) 763.
[4] F. Légaré, K.F. Lee, I.V. Litvinyuk, P.W. Dooley, S.S. Wesolowski, P.R. Bunker, P. Dombi, F. Krausz, A.D. Bandrauk, D.M. Villeneuve, P. Corkum, Phys. Rev. A 71 (2005) 13415.
[5] L. Lammich, H. Buhr, H. Kreckel, S. Krohn, M. Lange, D. Schwalm, R. Wester, A. Wolf, D. Strasser, D. Zajfman, Z. Vager, I. Abril, S. Heredia-Avalos, R. Garcia-Molina, Phys. Rev. A 69 (2004) 062904.
[6] G. Osmann, P.R. Bunker, P. Jensen, W.P. Kraemer, Chem. Phys. 225 (1997) 33.
[7] A. Baer, M. Grieser, L. Knoll, J. Levin, R. Repnow, D. Schwalm, Z. Vager, R. Wester, A. Wolf, D. Zajfman, Phys. Rev. A 59 (1999) 1865.
[8] L. Lammich, Diploma thesis, Faculty for Physics and Astronomy, Ruprecht-Karls-University, Heidelberg, 2001.
[9] H. Lin, W. Thiel, S.N. Yurchenko, M. Carvajal, P. Jensen, J. Chem. Phys. 117 (2002) 11265.
[10] S.N. Yurchenko, M. Carvajal, P. Jensen, H. Lin, J. Zheng, W. Thiel, Mol. Phys., 103 (2005) 359.
[11] P. Jensen, J. Mol. Spectrosc. 128 (1988) 478.
[12] H.-G. Yu, T.J. Sears, J. Chem. Phys. 117 (2002) 666.
[13] P.R. Bunker, W.P. Kraemer, V. Špirko, J. Mol. Spectrosc. 101 (1983) 180.
[14] X. Huang, S. Carter, J. Bowman, J. Chem. Phys. 118 (2003) 5431.